Draft version February 1, 2008
Preprint typeset using LaTeX style emulateapj v. 10/09/06

SPITZER OBSERVATIONS OF TRANSIENT, EXTENDED DUST IN TWO ELLIPTICAL GALAXIES: NEW EVIDENCE OF RECENT FEEDBACK ENERGY RELEASE IN GALACTIC CORES

Pasquale Temi[1,2], Fabrizio Brighenti[3,4], William G. Mathews[3]

Draft version February 1, 2008

ABSTRACT

Spitzer observations of extended dust in two optically normal elliptical galaxies provide a new confirmation of buoyant feedback outflow in the hot gas atmospheres around these galaxies. AGN feedback energy is required to prevent wholesale cooling and star formation in these group-centered galaxies. In NGC 5044 we observe interstellar (presumably PAH) emission at 8 μm out to about 5 kpc. Both NGC 5044 and 4636 have extended 70 μm emission from cold dust exceeding that expected from stellar mass loss. The sputtering lifetime of this extended dust in the $\sim$ 1keV interstellar gas, $\sim 10^7$ yrs, establishes the time when the dust first entered the hot gas. Evidently the extended dust originated in dusty disks or clouds, commonly observed in elliptical galaxy cores, that were disrupted, heated and buoyantly transported outward. The surviving central dust in NGC 5044 and 4636 has been disrupted into many small filaments. It is remarkable that the asymmetrically extended 8 μm emission in NGC 5044 is spatially coincident with Halpha+[NII] emission from warm gas. A calculation shows that dust-assisted cooling in buoyant hot gas moving out from the galactic core can cool within a few kpc in about $\sim 10^7$ yrs, explaining the optical line emission observed. The X-ray images of both galaxies are disturbed. All timescales for transient activity – restoration of equilibrium and buoyant transport in the hot gas, dynamics of surviving dust fragments, and dust sputtering – are consistent with a central release of feedback energy in both galaxies about 10^7 yrs ago.

Subject headings: galaxies: elliptical and lenticular; galaxies: ISM; infrared: galaxies; infrared: ISM

1. INTRODUCTION

In a recent survey of elliptical galaxies observed with the *Spitzer* telescope we found spatially extended cold interstellar dust emitting at 70 μm in a significant fraction of our sample (Temi, Brighenti & Mathews 2007). A few unusual galaxies in our sample, having atypically large and massive dust lanes that often dominate the optical image, probably acquired their dust and cold gas from a merger. However, some optically normal elliptical galaxies also contain extended cold dust, such as the two galaxies we discuss here, NGC 5044 and 4636. Evidently, the source of this dust is internal, not from mergers. Since this dust is thought to be in direct contact with the hot, virialized interstellar gas ($kT \sim 1$ keV), it has a short lifetime ($\sim 10^7$ yrs) to sputtering destruction by thermal ions. Consequently, this dust is a spatial tracer of extremely transient events that recently occurred on kpc scales. Both galaxies are extended at 70 μm, but NGC 5044 is also extended at 8 μm in a manner similar to the highly asymmetric optical line emission from warm gas in this galaxy. The temperature of the warm gas is maintained by photoionization by UV radiation from hot post-asymptotic giant branch (AGB) stars and radiation of optical line emission; the dust is heated by starlight and hot thermal electrons and cooled by infrared emission.

As we proposed in Temi, Brighenti & Mathews (2007), current evidence is consistent with an internal origin for this dust, and we hypothesize that dust has been buoyantly transported from the galactic cores out to several kpc following a feedback heating event. In both galaxies small, disorganized fragments of optically absorbing dusty gas are visible within the central $\sim$100 parsecs, further evidence of a recent central energy release. In addition, *Chandra* X-ray images reveal that the extended hot interstellar gas in both galaxies is undergoing short-term gasdynamical activity. All this information converges to confirm the transient state of affairs in these galaxies. In particular, the association of interstellar PAH emission (from polycyclic aromatic hydrocarbon molecules) and warm gas ($T \sim 10^4$ K) in NGC 5044 indicates that we may be viewing this galaxy at a rare moment immediately following a release of energy near the central black hole. This type of central feedback energy release, thought to be caused by the accretion of a small mass of gas into the central black hole, has been proposed as a likely solution of the so-called cooling flow problem. In the following we adopt distances of 15 Mpc ($1' = 4.36$ kpc) for NGC 4636 and 33 Mpc ($1' = 9.60$ kpc) for NGC 5044 (Tonry et al. 2001).

2. IMAGES OF NGC 5044 AND NGC 4636

Figures 1 and 2 show *Spitzer* images of NCC 5044 and NGC 4636 at 160, 70, 24, and 8 μm. The 8-4.5 μm images are differences of *Spitzer* images at 8.0 and 4.5 μm. Details of the acquisition and reduction of far-infrared data at 24, 70 and 160 μm are described in Temi, Brighenti & Mathews (2007). These data were obtained with the Multiband Imager Photometer (MIPS) (Rieke et al. 2004) on the *Spitzer* Space Telescope. Both NGC 5044 and 4636 are detected at 160 μm, but neither image can be distinguished from a point source. However, as we illustrate in Figure 10 of Temi, Brighenti & Mathews (2007), at 70 μm both NGC 5044 and 4636 are clearly extended beyond the MIPS point response function.

[1] Astrophysics Branch, NASA/Ames Research Center, MS 245-6, Moffett Field, CA 94035.
[2] SETI Institute, Mountain View, CA 94043; and Department of Physics and Astronomy, University of Western Ontario, London, ON N6A 3K7, Canada. ptemi@mail.arc.nasa.gov
[3] University of California Observatories/Lick Observatory, Board of Studies in Astronomy and Astrophysics, University of California, Santa Cruz, CA 95064 mathews@ucolick.org
[4] Dipartimento di Astronomia, Università di Bologna, via Ranzani 1, Bologna 40127, Italy fabrizio.brighenti@unibo.it

Mid-infrared data at 3.6, 4.5, 5.8 and 8.0 μm for NGC 4636 were obtained using the Infrared Array Camera (IRAC) onboard *Spitzer* under the guaranteed time program (PID 69) led by PI G. Fazio (Fazio et al. 2004). NGC 4636 was observed for 60 seconds on each of the four IRAC wavelength channels. NGC 5044 was observed during an IRAC calibration program (PID 1160, PI: W. T. Reach). Images of NGC 5044 at each of the four IRAC bandpasses were recorded at 5 different positions slightly offset from the galaxy center. Observations at each position were acquired using a five position gaussian dither parameter with an integration time of 12 seconds per frame. Thus, the total on target integration time at IRAC wavelengths was 300 seconds. For all wavelengths and with both MIPS and IRAC, full coverage imaging was obtained for all observations with additional sky coverage to properly evaluate the background emission. We used the Basic Calibrated Data (BCD) products from the Spitzer Science pipeline (version 13.2) to construct mosaic images when necessary. Pipeline reduction and post-BCD processing using the MOPEX software package provide all necessary steps to process individual frames: dark subtraction, flat-fielding, mux-bleed correction, flux calibration, correction of focal plane geometrical distortion, and cosmic ray rejection.

Also shown in Figures 1 and 2 are images of the Hα+[NII] emission from the warm gas in NGC 5044 (isophotes) and 4636 (gray scale). The panels at the lower right in both figures illustrate isophotes of the X-ray images of the same central regions of both galaxies, produced from data in the *Chandra* archives, superimposed on optical images from the Digital Sky Survey.

The Hα+[NII] image of NGC 5044 is quite unusual, with extensions toward the East, North and (especially) to the South. These warm gas features are obviously unrelated to the underlying stellar distribution. The Hα+[NII] image in NGC 4636 is more compact, but nevertheless exhibits irregularities in the outer regions. The radial velocities of the warm gas in both galaxies determined from slit spectra show highly irregular activity of $\pm \sim 150$ km s^{-1} on scales of ~ 1 kpc that are unrelated to the bulk motion of the stars (Caon et al. 2000). These quasi-random velocities are consistent with the disordered spatial appearance of the warm gas.

3. EXCESS DUST IN NGC 5044 AND 4636 AND ITS ORIGIN

Recent studies of mid-infrared *Spitzer* IRS spectra of elliptical galaxies indicate that most of the emission shortward of 8 μm is photospheric, while emission in the 8-20 μm region is from circumstellar dust around mass-losing red giant stars (Bregman, Temi & Bregman 2006; Bressan et al. 2006). In addition, Temi, Brighenti & Mathews (2007) find a tight correlation between fluxes at 24 μm from *Spitzer* MIPS data and optical B-band fluxes, suggesting that circumstellar dust also dominates at this wavelength. But MIPS fluxes from elliptical galaxies at 70 and 160 μm are uncorrelated with optical fluxes from starlight, so we regard this colder dust as truly interstellar. It is remarkable that the fluxes at 70 and 160 μm vary by factors of 30-100 among galaxies with similar optical fluxes. Some elliptical galaxies with large 70 and 160 μm fluxes contain very extended, multi-kpc disks of cold, dusty gas consistent with the strength and spatial extent of the 70 μm image. Evidently, these galaxies have experienced an unusual major merger with a gas-rich spiral. However, a few optically normal elliptical galaxies, including NGC 5044 and 4636, also show unexpected large 70 and 160 μm fluxes with 70 μm emission extended well beyond the MIPS point response function.

Because the 8-24 μm spectrum of elliptical galaxies is dominated by circumstellar dust in outflowing stellar winds, some internally produced dust is expected when this dust moves into the interstellar environment, where it is heated by diffuse starlight to much lower temperatures and radiates in the far-infrared. In Temi, Brighenti & Mathews (2007) we describe a simple steady state model in which interstellar dust is continuously produced by normal mass loss from a single population of evolving stars and continuously destroyed by ion sputtering. A far-infrared spectral energy distribution (SED) can be calculated assuming a power-law initial grain size distribution $\propto a^{-3.5}$ in $0 < a < a_{max}$. This grain size distribution is normalized so that $\delta = (1/150)z(r)$ is the ratio of dust to gas mass in the circumstellar outflows where $z(r) \approx (r/R_e)^{-0.207}$ is a typical radial variation of the metal abundance (in solar units) in elliptical galaxies (Arimoto et al. 1997). We assume amorphous silicate grains and compute the temperature of each dust grain. The grain production rate is proportional to the local stellar density and the specific stellar mass loss rate for an old stellar population $\alpha_* = \dot{M}_*/M_* = 4.7 \times 10^{-20}$ s^{-1} (Mathews 1989). The sputtering rate of the grains is determined by the local density and temperature in the hot gas as determined from X-ray observations. The total galactic SED is found by integrating the dust emission over the steady state dust size distribution and galactic radius. We show in Figure 11 of Temi, Brighenti & Mathews (2007) that the far-infrared SED at 70 and 160 μm observed in at least a few galaxies – such as NGC 1399, 1404 and 4472 – can be fully explained by this type of normal stellar mass loss. Elliptical galaxies that agree with our steady state dust model are among those with the lowest 70 and 160 μm luminosities.

However, as illustrated in Figure 3, the 70 and 160 μm fluxes of both NGC 5044 and 4636 are far in excess of our predicted steady state SED. (The 24 μm flux shown in Figure 3 is circumstellar and is unrelated to our SED model.) The mass and spatial extent of the "excess" interstellar dust in these galaxies can be estimated using our steady state model but artificially increasing the stellar mass loss rate α_* within radius r_{ex}. Increasing α_* by some factor f_α increases the mass of interstellar dust and r_{ex} can be adjusted until the mean grain temperature approximately fits the 70 μm/160 μm flux ratio observed in each galaxy. Interstellar dust is heated by starlight and by inelastic collisions with thermal electrons. Since the mean intensity of starlight and the electron density both decrease with galactic radius, the dust temperature T_d also decreases, so r_{ex} can be adjusted to change mean dust grain temperature $\langle T_d \rangle$ and therefore the 70 μm/160 μm flux ratio. These values of f_α, r_{ex} and the excess dust mass estimated from them are only approximations, since it is unlikely that the radial distribution of the excess non-stellar dust exactly follows the stellar density profile, but with a sharp truncation at r_{ex}.

Each panel of Figure 3 shows three combinations of f_α and r_{ex}, holding $a_{max} = 0.3\mu$m constant. The best-

fitting SED for the extra dust in NGC 5044 and 4636, shown by dotted lines in both panels, corresponds respectively to a mass of excess dust of 1.5×10^5 and 1.1×10^5 $M_\odot$. The physical size of this dust, $r_{ex} \sim 4 - 5$ kpc, is comparable to or exceeds the 70 μm point response function for both galaxies. We propose below that r_{ex} is limited by the sputtering time in buoyant dusty gas flowing from galaxy cores.

We argue in Temi, Brighenti & Mathews (2007) that the incidence of (otherwise normal) elliptical galaxies with excess dust emission at 70μm exceeds the fraction of ellipticals that are likely to have experienced mergers with dusty gas-rich (dwarf) galaxies within a typical dust sputtering time $t_{sput} \approx 10^7$ yrs, evaluated a few kiloparsecs from the galactic center. In addition, since t_{sput} is somewhat less than the typical free fall time from several effective radii, if the extended dust were a result of merging, ellipticals having far-infrared excesses should contain evidence of the merging galaxies within their optical images, but this is not observed. The mean stellar ages of elliptical galaxies can be measured from the strength of Balmer line absorption features. Annibali et al. (2006) find a stellar age of 13.5 ± 3.6 Gyrs for NGC 4636 but the age for NGC 5044 (14.2 ± 10. Gyrs) is indeterminate because the Balmer absorption is masked by the much stronger interstellar Balmer emission in this galaxy. The optical colors of both galaxies also seem normal, $B - V \approx 0.97 - 1.06$ (Poulain 1988; Poulain & Nieto 1994). Finally, the stellar velocity dispersion and rotation are largely normal for both galaxies[1] , with no kinematical indication of an alien merging stellar system (Caon, Macchetto, & Pastoriza, 2000). We conclude there is no optical evidence in either galaxy of a merger event during the previous $\sim 10^8$ yrs.

In Temi et al. (2003) we first discovered excess dust at 60, 90 and 180 μm in NGC 4636 from observations with the *Infrared Space Observatory* (ISO) and proposed that the short-lived dust resulted from a recent merger. However, now that the age of the stars in NGC 4636 has been found to be very old and the dust is known to be extended, our earlier merger explanation is untenable. Instead, as discussed in Temi, Brighenti & Mathews (2007), we now propose that the extended excess dust seen in both NGC 4636 and 5044 and other similar galaxies has been buoyantly transported from the galactic core to several kpc following a heating event near the central black hole.

Galactic cores are a natural source of dust. Mathews & Brighenti (2003) showed that the $\sim 100 - 300$kpc-sized nuclear disks that are often observed in the nuclei of elliptical galaxies (e.g. Lauer et al. 2005) can result from stellar mass loss within the innermost ∼1 kpc at a rate $\dot{M}_1 \approx \alpha_* M_1 \approx 0.1$ $M_\odot$ yr^{-1}, where $M_1 \sim 5 \times 10^{10}$ $M_\odot$ is the stellar mass in the central kpc.

In the Appendix of Temi et al. (2007) we showed that the excess far-infrared emission at 70 and 160 μm cannot arise from these small nuclear dust disks/clouds but must come from dust distributed 5-10 kpc into the hot gas.[2] We hypothesized that the spatially extended dust has its origin in the nuclear disks/clouds that are disrupted and buoyantly transported to large radii in the hot gas as a result of intermittent AGN-type heating in the galactic core. The mass of excess extended dust, $\sim 10^5$ $M_\odot$, is consistent with this.

Consider for example the time t_{disk} required to form an optically obscuring dusty disk of radius $r \sim 300$ pc. To block starlight, the column density in the disk must exceed about $N \sim 10^{21} N_{21}$ cm^{-2}, assuming solar abundance. So the total mass of an optically dark disk of radius r is at least $M_{disk} \approx [5\mu/(2+\mu)] m_p N \pi r^2 \approx 3 \times 10^7 N_{21} r_{300}^2$ $M_\odot$ where r_{300} is the disk radius in units of 300 parsecs and $\mu = 0.61$ is the mean molecular weight. [This disk mass is consistent with the upper limit to the HI mass in NGC 4636 of 1.1×10^8 $M_\odot$ established by Krishna Kumar & Thonnard (1983).] The time for stellar mass loss (within the central kpc) to form such an obscuring disk, $t_{disk} \approx M_{disk}/\dot{M}_1$, is only $t_{disk} \approx 3 \times 10^7 N_{21} r_{300}^2$ yrs, similar to the buoyant rise time in the hot gas. For a dust to gas mass ratio $\delta \sim 0.01$, these disks should contain about 3×10^5 $M_\odot$ of dust, which is very similar to the dust we observe in NGC 5044 and 4636 in excess of our steady state model.

To support this hypothesis further, we show in Figure 4 *Hubble Space Telescope* images of the central $\sim 1 - 2$ kpc in NGC 5044 and 4636. Small, chaotically arranged dusty fragments are visible against the stellar background in both galaxies. The dense gas in these fragments is clearly in a highly transient state, dynamically orbiting in the galactic potential out to a few kpc where the freefall time is $\sim 10^7$ years. It is very unlikely that these relatively large optically obscuring clouds can be interpreted as infalling dust just after being ejected from stars. The radius of individual optically dark fragments in Figure 4 is about 10 parsecs, which translates to a dust mass $\sim 3 \times 10^4$ $M_\odot$ far in excess of that from a single star or from a hypothetical agglomeration of several stellar outflows during the short freefall time. We propose instead that these dusty regions are fragments of a central, more organized disk-like structure that was disrupted about 10^7 yrs ago by an AGN-related energy release. While it may seem unlikely that dense fragments can result from an AGN energy release and be accelerated outwards in this quasi-coherent manner, we appeal to studies of Seyfert galaxies where similar large and dense clouds are accelerated in just this manner by non-thermal, radio-emitting outflows (e.g. Whittle, et al. 2005).

As soon as a dusty disks are destroyed by a significant release of AGN energy, another disk begins to form. The

[1] NGC 4636 does have a few minor peculiarities. Slit spectra of Caon, Macchetto & Pastoriza (2000) indicate that the mean stellar radial velocity has a broad central *minimum* at position angle 117^o, but not in other directions. Also, for its luminosity and central stellar velocity dispersion NCC 4636 has an unusually low near-IR stellar surface brightness, causing it to deviate from the fundamental plane for galaxy cores (Ravindranath, et al. 2001).

[2] Cold dust inside dense, optically thick nuclear disks/clouds is self-shielded and cannot be heated by the diffuse stellar UV radiation from hot post-AGB stars. The apparent longevity of these optically thick clouds ($\sim 10^7$ yrs) suggests that heating by thermal electrons in the adjacent hot gas is also suppressed. Evidently magnetic fields (tangent to the surface of the spinning disks) are sufficient to restrict thermal conduction. However, when the dusty gas is heated and dispersed by an AGN explosion, some of the dust is directly exposed to diffuse galactic UV and hot thermal electrons that heat the dust to radiate much more efficiently at infrared wavelengths. But when the same mass of dust is contained in dense, self-shielding central disks, its infrared luminosity is unobservably low.

fragments visible in Figure 4 indicate that some fraction of the disk received kinetic energy but was not irreversibly heated by the explosive AGN event. Therefore the next generation disks in these galaxies will be formed out of these denser remnants of the previous disk and new dust that is continuously ejected from red giant stars in the galactic core. At present it is impossible to know what fraction of disk material is heated to supervirial (buoyant) temperatures and what fraction remains in the fragments visible in Figure 4. Nor is it clear at present what limits the maximum amount of dusty cold gas that resides in central disks/clouds.

The only signs of current nuclear activity in NGC 5044 and 4636 are small, weak non-thermal GHz nuclear radio sources. There is no evidence of disk or Bondi type accretion. For example, from Chandra observations of NGC 4636 Loewenstein et al. (2001) determined that the accretion onto the 8×10^7 $M_\odot$ central massive black hole in this galaxy is less than $3 \times 10^{-8} L_{edd}$ and less than 6×10^{-4} of the spherical Bondi accretion rate. The general absence of mass accretion in supermassive nucelear black holes in elliptical galaxies is consistent with models in which most of their mass was acquired during a short-lived early evolutionary phase (e.g. Hopkins, Narayan, & Hernquist 2006). The AGN-type energy releases in NGC 5044 and 4636 required in our interpretation must also be sufficiently short-lived or radiatively unremarkable.

4. PAH EMISSION FROM NGC 5044

Perhaps the most dramatic illustration of extended dust in NGC 5044 is the difference image between IRAC wavelengths 8 and 4.5 μm shown in Figure 1 and its striking similarity to that of the warm gas emission in Hα+[NII]. The 8-4.5 μm difference image is constructed by subtracting a properly normalized 4.5 μm image from the 8 μm image. Emission at 4.5 μm is due largely to stellar photospheres while both photospheric and circumstellar emission contribute at 8 μm – but the 8 μm image may also contain interstellar emission from hot dust emission or the strong 7.7 μm PAH emission feature. When the two images are subtracted, both the stellar and circumstellar emission are canceled, and only emission from the faint interstellar dust emission remains. Our subtraction process in NGC 5044 was based on visual examination of the surface brightness Σ in the difference image $\Sigma_{8.0} - F\Sigma_{4.5}$ where the subscripts refer to the IRAC wavelengths and F is a variable parameter. As F was varied, the stellar surface brightness of the difference image of the stellar emission passes through a cancellation when $F = \Sigma_{8.0}/\Sigma_{4.5}$. In this process particular attention was paid to the residual stellar brightness in the region along the Hα plume about 3-5 kpc south of the galactic center. The value of F at which the stellar contributions at 8.0 and 4.5 microns outside the plume region are equalized depends on the galactic radius in NGC 5044. The 8-4.5 μm image of NGC 5044 shown in Figure 1 corresponds to $F \approx 0.52$ where the stellar emission near the plume canceled and the faint residual interstellar features are revealed. Our value of F is almost identical to $F = 0.526$ which is the flux ratio $F_{8.0}/F_{4.5}$ of a 10 Gyr old solar abundance single stellar population estimated by Piovan et al. (2003), who include both photospheric and circumstellar infrared emission. In our difference image of NGC 5044 the interstellar emission exhibits the same extended features toward the north and south that are so prominent in the Hα+[NII] isophotes. We estimate that the total luminosity of the 8 μm component is about 4 percent of the total interstellar far-infrared luminosity longward of 24 μm, this is similar to the PAH emission fraction observed in Milky Way sources.

The residual interstellar feature in NGC 5044 could be due to the strong PAH emission band at 7.7 μm or to hot dust emission from small, stochastically heated dust grains, in some proportion. Dust with temperatures approaching 10^3 K could be heated by an intense beam of optical-UV radiation from the galactic center along the direction of the plume. However, to our knowledge normal elliptical galaxies with abnormally UV-bright nuclei, when viewed along such beams, are not commonly observed. In principle, thermal excursions of small grains recently heated by individual photons or electrons could explain the diffuse 8 μm emission. For example, this process is thought to explain the diffuse near-infrared dust emission often observed in planetary nebulae (e.g. Phillips & Ramos-Larios 2006). During the short-lived stages as the dusty hot gas in the southerly plume of NGC 5044 cools, the electron density increases and stochastic heating of small grains by electron encounters may increase. However, in situations where stochastically heated dust emission dominates, the infrared continuum generally increases from 8 toward longer wavelengths since a larger fraction of small grains can be momentarily heated to lower temperatures that radiate at longer wavelengths (e.g. Draine & Anderson 1985). But this increase is not observed in spectra of normal elliptical galaxies taken with the *Spitzer* Infrared Spectrograph (IRS) (e.g. Bregman, Temi & Bregman 2006). Our 24 μm image of NGC 5044 (not shown in Figure 1) shows no evidence of asymmetrically extended emission similar to the optical line emission.

If the extended 8-4.5 μm feature visible to the south in Figure 1 were due to transient thermal excursions of small grains, this feature would be even more pronounced in a 24-4.5 μm difference image. To explore this possibility, we spatially degraded the 4.5 μm image to the PSF of the 24 μm image and varied the flux ratio to cancel the stellar and circumstellar emission at both wavelengths. We see no non-stellar residual interstellar enhancement in the 24-4.5 μm image of NGC 5044 that is geometrically similar to the plume extension visible in optical emission and the 8.0-4.5 μ difference image. The absence of extended emission in the 24-4.5 μm image of NGC 5044 is therefore a strong argument for PAH emission at 8 μm and for the relative unimportance of thermal excursions in the mid-infrared dust SED in this galaxy. An IRS spectrum of NGC 5044 has been taken but it is not currently available in the *Spitzer* archive, although the extended interstellar emission in Figure 1 may be too faint to be easily visible as PAH emission features in the spectrum.

In the following discussion we adopt a PAH interpretation of the 8 μm interstellar features in NGC 5044, but the precise identification of this dust-related interstellar emission is not central to our main arguments. It is unclear if the PAH is located in the warm gas or is in the hot interstellar gas where its expected lifetime is short but its modes of excitation and emission might be more easily excited.

Evidence of PAH emission in *Spitzer* IRS spectra of elliptical or other early type galaxies is rare and has only been found in a few unusual early-type galaxies that have starburst activity in massive cold disks: NGC 4550, NGC 4435 (Bressan et al. 2006; both are SB0 galaxies) and NGC 4697 (Bregman, Bregman & Temi 2006; an E6 galaxy with a dust lane that may be an S0).

It is unclear at present if the extended 70 μm emission also shows the same feature to the south of NGC 5044. When the 8-4.5 μm feature is convolved with the PRF of the 70 μ filter, this southern extension largely disappears.

The very elongated Hα+[NII] image in NGC 5044 is unusual – perhaps the only other elliptical galaxy that is known to have a similar feature (unrelated to large disks of cold gas) is NGC 5813 (Goudfrooij et al. 1994). In normal galaxies without extended dust or warm gas features, all the warm gas is expected to result from stellar mass loss and is generally visible only within the central kpc. Gas ejected from evolving stars at a rate $\alpha_* M_*$ (where $\alpha_* = 4.7 \times 10^{-20}$ s^{-1}) cannot accumulate in the warm gas phase indefinitely since otherwise after $\sim 10^5$ yrs the Hα+[NII] flux would exceed values commonly observed in most elliptical galaxies. We conclude therefore that the warm line-emitting gas thermally merges with the hot ($T \sim 10^7$ K) interstellar gas in this time (Mathews & Brighenti 1999). Therefore the extended warm gas observed in NGC 5044 is very transitory, although the PAHs and warm gas may be continuously supplied for a longer time $\sim 10^7$ years as gas cools in the buoyant dusty plume.

5. BUOYANT DUST OUTFLOW IN NGC 5044

Two questions come to mind about buoyant dust transport. Can dust grains survive sputtering destruction during their buoyant journey out to ~ 5 kpc, the approximate extent of the Hα+[NII] and PAH emission features in NGC 5044? Can the dust also cool (some of) the buoyant gas to create the warm gas that emits Hα+[NII]? To answer these questions we consider a simple model in which gas is assumed to be heated at some small radius r_0 in NGC 5044 and remains in hydrostatic equilibrium as it moves buoyantly out at velocity v. For simplicity we assume v is constant since the buoyant velocity depends on the size of the buoyant region and other uncertain parameters. After the gas is heated at radius r_0 it has an electron density n that is lower by a factor $\Delta < 1$ than the local ambient density of the hot gas, i.e. $n(r_0) = \Delta \hat{n}(r_0)$. In this Section variables with hats refer to the (unheated) ambient hot gas in NGC 5044. The density and temperature profiles in NGC 5044, found from X-ray observations (i.e. Buote et al. 2003), can be approximated with the following expressions:

$$\hat{n} = \frac{0.065}{r_{kpc}^{1/2}[1+(r_{kpc}/9.5)^{1.05}]} + \frac{0.002}{[1+(r_{kpc}/30.5)^{3/2}]} \quad \mathrm{cm}^{-3} \tag{1}$$

and

$$\hat{T} = \frac{10^7}{[F(r_{kpc})^{-3} + G(r_{kpc})^{-3}]^{1/3}} - 0.12e^{-(r_{kpc}/1.5)} + 3\times 10^6 \quad \mathrm{K} \tag{2}$$

where

$$F(r_{kpc}) = 0.85 + 0.95(r_{kpc}/30)^2 \tag{3}$$

and

$$G(r_{kpc}) = 1.64(r_{kpc}/30)^{-0.10}. \tag{4}$$

For simplicity we assume that the grains have a single initial radius $a(r_0)$ and, as they move buoyantly outward, are sputtered at a rate given by

$$\frac{da}{dr} = -\frac{3.2\times 10^{-18} n_p}{v}\left[1+\left(\frac{2\times 10^6 \mathrm{K}}{T}\right)^{2.5}\right]^{-1} \quad \mathrm{cm\ cm}^{-1} \tag{5}$$

(Tsai & Mathews 1995) where $n_p = 0.83 n_e$ is the proton density. As the buoyant gas flows out in local pressure equilibrium, $P = \hat{P}$, its temperature follows an adiabat ($T \propto P^{(\gamma-1)/\gamma}$ with $\gamma = 5/3$) modified by radiative losses,

$$\frac{dT}{dr} = \frac{2T}{5\hat{P}}\left[\frac{d\hat{P}}{dr} - \frac{1}{v}\left(\frac{\mu\hat{P}}{kT}\right)^2(\Lambda_{gas}+\Lambda_{dust})\right]. \tag{6}$$

The first term in square brackets describes the adiabatic cooling of the buoyant gas as it expands, continuously adjusting to the decreasing ambient pressure as it moves out in the hot gas atmosphere of NGC 5044. The second term is the intrinsic cooling that occurs in the buoyant gas due to standard radiative losses with coefficient $\Lambda_{gas}(T)$ (e.g. Sutherland & Dopita 1993) and due to the absorption of thermal electrons by inelastic collisions with the grains,

$$\Lambda_{dust} = \frac{9}{8}\frac{(2+\mu)}{5\mu}\frac{\delta m_p}{\rho_g}\left(\frac{8}{\pi m_e}\right)^{1/2}\frac{(kT)^{3/2}}{a} \quad \mathrm{ergs\,cm^3\ s^{-1}} \tag{7}$$

(Mathews & Brighenti 2003). We assume a uniform dust mass to gas mass ratio of $\delta = 0.015$ in the initial gas, similar to that in Milky Way gas. The mass density of the grain material $\rho_g = 3.3$ g cm^{-3} is appropriate for amorphous silicates.

The solution to these equations shown in Figure 5 corresponds to the following (somewhat arbitrary) parameters: $r_0 = 200$ pc, $\Delta = 0.15$, $a(r_0) = 1\mu$m, and $v = 400$ km s^{-1}. The upper panel of Figure 5 shows Chandra observations of the hot and cold temperature phases in NGC 5044 (Buote et al. 2003). The solid lines in the upper two panels show the temperature and density profiles of the cooler, dense phase $\hat{T} \equiv T_c(r)$ and the long-dashed lines show the buoyant evolution of dust-free gas heated by a factor Δ^{-1} at r_0. The short-dashed lines in Figure 5 show the trajectory of the same heated gas but with a uniform admixture of dust at a fraction $\delta = 0.015$ of the gas mass. It is seen that the buoyant gas does in fact cool to low temperatures ($T \ll \hat{T}$) at $r \approx 5$ kpc similar to the extent of the southern warm gas feature observed in NGC 5044. The dust-assisted cooling occurs in $\sim 10^7$ yrs even though the buoyant gas was initially hotter than the ambient gas $\hat{T}$; the bottom panel in Figure 5 shows that dust cooling dominates at every radius in the dusty buoyant gas. Evidently, the PAH emission observed comes from residual dust fragments diminished by sputtering. Perhaps the least satisfactory aspect of this approximate calculation is the rather high value of the buoyant velocity required to reach ~ 5 kpc in $\sim 10^7$ yrs, $v = 400$ km s^{-1}, which nearly approaches the sound speed $c_s = (\gamma k\hat{T}/\mu m_p)^{1/2} = 480(\hat{T}/10^7\ \mathrm{K})^{1/2}$ km s^{-1}.

This suggests that the buoyantly heated gas may have received momentum from a jet emerging from the central black hole.

Considering the many uncertainties involved, it seems plausible from Figure 5 that the peculiar asymmetric extensions of warm gas in NGC 5044 can be formed by dust-assisted cooling of buoyant flow. Buoyant gas that was heated less at r_0 (i.e. $\Delta > 0.15$) or which contains a locally higher dust density will cool at smaller radius, explaining the full extent of the warm gas feature in NGC 5044. The enhanced soft X-ray emission extending southward in the general direction of the plume (Figure 1) could be due to enhanced emission from cooling (and therefore denser) hot gas. Indeed, we note that the cooling in Figure 5 occurs on a timescale $\sim 10^7$ yrs consistent with other transient events in the hot gas in both NGC 5044 and 4636 which we discuss below.

6. CENTRAL OPTICAL AND X-RAY CAVITY IN NGC 4636

Optical line emission from warm gas in the central ~ 1 kpc of NGC 4636 and thermal X-ray emission from the hot gas both have a small cavity slightly displaced from the galactic center [3] (Figure 6). Demoulin-Ulrich et al. (1984), Buson et al. (1994) and Zeilinger et al. (1996), all noticed a nearly circular hole of radius $r_{hole} = 1.7'' = 120$ parsecs in the Hα+[NII] image that is clearly visible in Figure 6 just NE of the galactic center. At the right in Figure 6 is an X-ray image taken from the *Chandra* archives. Superimposed on the X-ray image are approximate contours showing the radio jets as observed at 1.4 GHz by Stanger & Warwick (1986) and at 5 GHz by Birkinshaw & Davies (1985). The (steep spectrum) double radio jets are about 1 kpc long, oriented at position angle $\sim 45^o$. It is remarkable that the circular hole seen by the optical observers is also visible in the *Chandra* image. While the X-ray emitting gas (paradoxically) appears to have been disturbed very little by the radio lobes, the energy source that created the circular cavity to the NE has does not contain a significant non-thermal radio source of its own.

Assuming that the circular feature is formed by a point explosion, the energy required to form a hole of radius r_{hole} in the hot gas is $E \approx (3P/2\rho) \cdot \rho V_{hole} = 2\pi r_{hole}^3 P$, where $P = 1.9nkT$ is the local gas pressure. Using central values of the hot gas density n and temperature T from Allen et al. (2006), we estimate that the local gas pressure near the circular cavity is $P \approx 6.14 \times 10^{-10}$ dynes cm^{-2}. The energy required to form this hole is therefore $E \approx 200 \times 10^{51}$ ergs. This energy far exceeds that of a single supernova, so the cavity was probably formed with energy released near the central black hole. Since the chaotic warm gas velocities observed by Caon, Macchetto & Pastoriza (2000) near the hole are $v \sim \pm 50 - 100$ km s^{-1}, the age of the hole cannot exceed $t_{hole} \approx 2r_{hole}/v \approx 2 \times 10^6/v_{100}$ yrs where v_{100} is the local warm gas velocity in units of 100 km s^{-1}. Evidently, the central AGN-black hole in NGC 4636 has been active during the last few million years.

7. TRANSIENT ACTIVITY IN THE HOT GAS

[3] The cavity is less visible in the emission line image shown in Figure 2 probably because of the gray-scale intensities adopted by Caon et al. (2000).

Unlike most other similar galaxy/groups, *XMM* X-ray spectra of the hot gas in the NGC 5044 group show that the hot gas within about 30 kpc from the central galaxy does not have a uniform temperature at each radius (Figure 5; Buote et al. 2003). In most galaxy groups and clusters the hot gas temperature rises from the center and peaks at about 0.1 of the virial radius, then decreases further out. The emission-weighted (single) temperature profile in NGC 5044 has a similar thermal structure. However, *XMM* spectra reveal that NGC 5044 contains an additional component of hotter gas in which the temperature *decreases* outward from the center (Buote et al. 2003) as shown by the long-dashed line in the top panel of Figure 5. Since this hotter (and therefore less dense) gas in NGC 5044 must be buoyant, it is natural to associate it with the dust-transporting regions discussed in the previous section. The "multi-phase" character of the X-ray spectrum of NGC 5044 is also evident from the hot gas density irregularities visible in the *Chandra* image (Fig. 1 of Buote et al. 2003) with isophotes shown in our Figure 1. It appears that the X-ray feature toward the south in NGC 5044 is roughly coincident with the Hα+[NII] and PAH extensions in that same region. The enhanced X-ray emission in this region may result from slightly denser gas that is undergoing dust-assisted cooling in the buoyant plume. Overall, observations indicate many dusty plumes in NGC 5044, but only the plume toward the south is currently producing warm gas out to ~ 5 kpc.

X-ray spectra and images of NGC 4636 also reveal evidence of recent, possibly somewhat more violent activity in this galaxy/group. *Chandra* observations presented by Jones et al. (2002) show a symmetric X-shaped parabolic pattern of enhanced emission, presumably caused by shock waves, that enclose cavities several kpc to the east and west of the galactic center. Jones el al. interpret this as the result of two symmetric and nearly simultaneous point explosions ($\sim 10^{57}$ ergs) offset from the galactic center that occurred about 3×10^6 yrs ago. No radio emission has been observed in these cavities which are somewhat misaligned from the current radio jets shown in Figure 6 (Birkinshaw & Davies 1985; Stanger & Warwick 1986).

The X-ray observations of NGC 4636 and their explanation do not necessarily require a (buoyant) mass outflow that could create the extended dust emission observed at 70μm. However, strong evidence for outflows in NGC 4636 is provided by the *XMM* spectra and images shown by O'Sullivan, Vrtilek and Kempner (2005). Their abundance map of NGC 4636 shows a patch of gas with high abundance about 25-30 kpc toward the southwest of the galactic core. O'Sullivan et al. interpret this as evidence of an older (collimated, plume-like) gas outflow that transported gas from the galactic center that was enriched by Type Ia supernovae. Consequently, there is now good X-ray evidence that the same kind of transient collimated outflow has occurred in both of these galaxies having extended far-infrared emission.

8. FINAL REMARKS

We discuss two optically normal elliptical galaxies, NGC 5044 and NGC 4636, in which we discovered spatially extended interstellar dust at 70μm. In NGC 5044 we observe asymmetrically extended interstellar 8μm

PAH emission associated with warm gas and extending about 5 kpc from the center of the galaxy. In view of the short sputtering lifetime for extended dust, $\sim 10^7$ yrs, and the commonplace optical appearance of both galaxies, we conclude that the extended dust observed cannot result from a recent merger with a gas-rich galaxy. The stellar morphologies, spectra, colors and old ages of these two galaxies appear to be normal with no evidence of an additional merger component. Instead, we propose that the extended excess dust is created by stellar mass loss in the central ~ 1 kpc and stored in small disks or clouds in the galactic cores. These disks are intermittently disrupted and heated by energy released by accretion onto the central black holes (AGN feedback). Finally, the heated dusty gas is buoyantly transported out to several kpc where it is observed. The physical extent of the extended dust is governed by the buoyant velocity and either the grain sputtering time or the dust-assisted cooling time, whichever is shorter.

X-ray observations of both NGC 5044 and 4636 show unusual, transient features consistent with recent energy releases in or near the galactic cores. Both galaxies show disorganized, highly fragmented optically visible dust clouds in the central 100-200 parsecs that are also highly transient. Finally, the timescales for all these processes are comparable to the sputtering lifetime of the extended dust, about 10^7 yrs.

We are particularly privileged to view NGC 5044 during a brief interval when asymmetric, radially extended 8μm PAH and Hα+[NII] emission is present in the outflowing gas. We explain this remarkable observation as a result of dust-assisted cooling in a buoyant plume of hot dusty gas. We show with a simple calculation that dust can cool buoyant gas to $\sim 10^4$ K which emits the optical emission lines observed. The warm gas phase is maintained in thermal equilibrium near $\sim 10^4$ K by radiative losses and UV heating from post-AGB stars. Based on the collective Balmer line luminosities of normal elliptical galaxies, we conclude that this warm gas can only last for $\sim 10^5$ yrs before it thermally melts into the dominant hot interstellar phase. Finally, the buoyant outflow described here is an essential feature of flows that successfully resolve the cooling flow problem with the outward transport of both mass and energy from the galactic core to large radii, i.e. a circulation flow (Mathews, Brighenti & Buote 2004).

This work is based on observations made with the Spitzer Space Telescope, which is operated by the Jet Propulsion Laboratory, California Institute of Technology, under NASA contract 1407. Support for this work was provided by NASA through Spitzer Guest Observer grant RSA 1276023. Studies of the evolution of hot gas in elliptical galaxies at UC Santa Cruz are supported by NASA grants NAG 5-8409 & ATP02-0122-0079 and NSF grant AST-0098351 for which we are very grateful.

REFERENCES

Allen, S. W., Dunn, R. H., Fabian, A. C., Taylor, G. B. & Reynolds, C. S. 2006, MNRAS, 272, 21
Annibali, F., Bressan, A., Rampazzo, R., Zeilinger, W. W. & Danese, L. 2006, A&A (in press) (astro-ph/0609175)
Arimoto, N., Matsushita, K., Ishimaru, Y., Ohashi, T. & Renzini, A. 1997, ApJ, 477, 128
Birkinshaw, M. & Davies, R. 1985, ApJ, 291, 32
Bregman, J. N., Temi, P. & Bregman, J. D. 2006, ApJ, 647, 265
Bregman, J. D., Bregman, J. N. & Temi, P. 2006, to appear in *The Spitzer Science Center 2005 Conference: Infrared Diagnostics of Galaxy Evolution*, (astro-ph/0604369)
Bressan, A. et al. 2006, ApJ, 639, L55
Buote, D. A., Lewis, A. D., Brighenti, F. & Mathews, W. G. 2003, ApJ, 594, 741
Buson, L. M. et al. 1993, A&A, 280, 409
Caon, N., Macchetto, D. & Pastoriza, M. 2000, ApJS, 127, 39
Demoulin-Ulrich, M. H., Butcher, H. R. & Boksenberg, A. 1984, ApJ, 285, 527
Draine, B. T. & Anderson, N. 1985, ApJ, 292, 494
Fazio, G. G. et al. 2004, ApJS, 154, 10
Goudfrooij, P., Hansen, L, Jorgensen, H. E., & Norgaard-Nielsen, H. U. 1994, A&AS, 105, 341
Hopkins, P. F., Narayan, R., Hernquist, L., 2006, ApJ, 643, 641
Jones, C., Forman, W., Vikhlinin, A., Markevitch, M., David, L., Warmflash, A., Murray, S., & Nulsen, P. E. J. 202, ApJ, 567, L115
Krishna Kumar, D. & Thonnard, N. 1983, AJ, 88, 260
Lauer, T., R. et al. 2005, AJ, 129, 2138
Loewenstein, M., et al. 2001, ApJ, 555, L21
O'Sullivan, E., Vrtilk, J. M. & Kempner, J. C. 2005, ApJ, 624, L77
Mathews, W. G. 1989, AJ, 97, 42
Mathews, W. G. & Brighenti, F. 2003, ApJ, 590, L5
Mathews, W. G. & Brighenti, F. 1999, ApJ, 526, 114
Mathews, W. G., Brighenti, F. & Buote, D. A. 2004, ApJ, 615, 662
Phillips, J. P. & Ramos-Larios, G. 2006, MNRAS, 368, 1773
Piovan, L, Tantalo, R.,& Chiosi, C. 2003, A&A, 408, 559
Poulain, P. 1988, A&AS, 72, 215
Poulain, P. & Nieto, J.-L. 1994, A&AS, 103, 573
Ravindranath, S. et al. 2001, AJ, 122, 653
Stanger, V. & Warwick, R. 1986, MNRAS, 220, 363
Sutherland, R. S. & Dopita, M. A. 1993, ApJS, 88, 253
Temi, P., Brighenti, F., & Mathews, W. G. 2007, ApJ (in press) (astro-ph/0701431)
Temi, P., Mathews, W. G., Brighenti, F., & Bregman, J. D. 2003, ApJ, 585, L121
Tonry, J. et al. 2001, ApJ, 546, 681
Tsai, J. C. & Mathews, W. G. 1995, ApJ, 448, 84
Whittle, M., Rosario, D. J., Silverman, J. D., Nelson, C. H. & Wilson, A. S. 2005, ApJ, 129, 104
Zeilinger, W. W. et al. 1996, A&AS, 120, 257

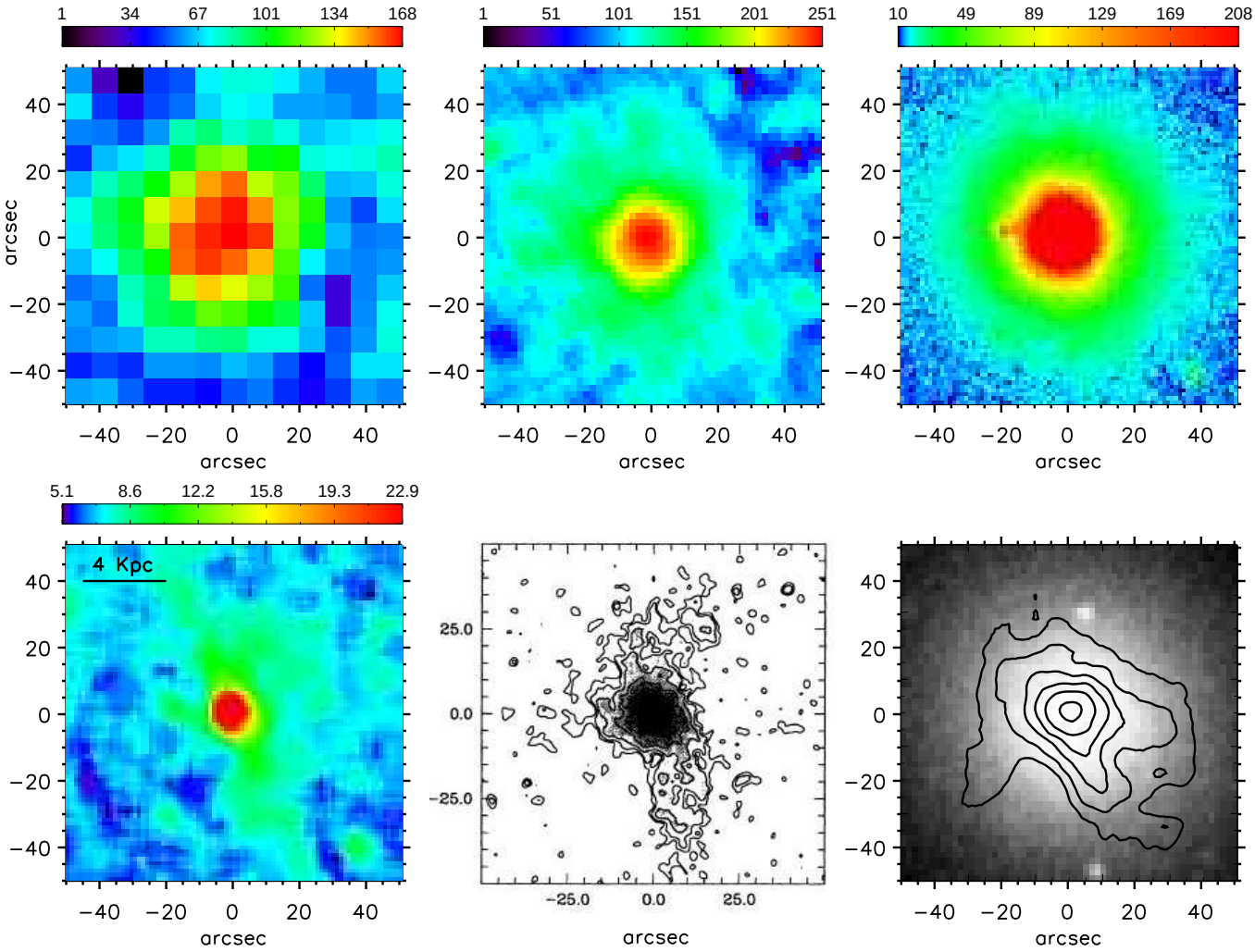

FIG. 1.— Comparison of optical, infrared and X-ray emission from NGC 5044. The physical scale is 160 parsecs/″. The top three panels from left to right show *Spitzer* images at (1) 160 μm, (2) 70 μm, and (3) 8 μm. A small source about 20″ to the East of the center of NGC 5044, is revealed in the 8 μm image. This source is coincident with a point-like source in the $B-I$ image of Goudfrooij et al. (1994) and appears as a background galaxy in the HST image. The second row of panels from left to right shows: (1) the difference image 8-4.5 μm, (2) isophotes of Hα+[NII] emission from warm gas in NGC 5044 taken from Goudfrooij et al. (1994) and (3) isophotes from the *Chandra* X-ray images superimposed on an optical image from the Digital Sky Survey. Surface brightness values in the color bars are presented in units of $\mu Jy/arcsec^2$.

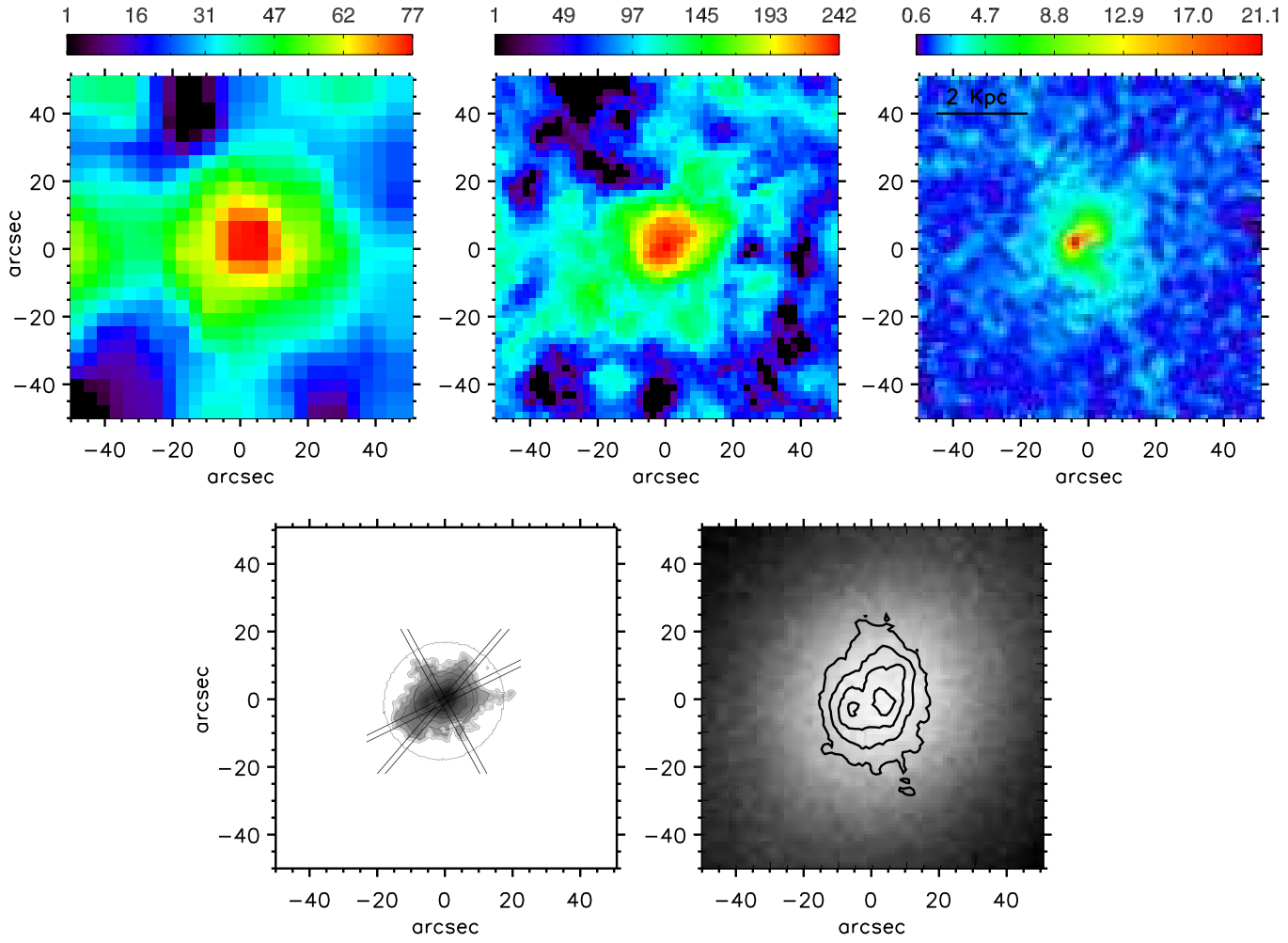

FIG. 2.— Comparison of optical, infrared and X-ray emission from NGC 4636. The physical scale is 73 parsecs/″. The top three panels from left to right show *Spitzer* images at (1) 160 μm, (2) 70 μm, and (3) the difference image 8-4.5 μm. Surface brightness values in the color bars are presented in units of $\mu Jy/arcsec^2$. The second row of panels from left to right shows: (1) isophotes of Hα+[NII] emission from warm gas in NGC 4636 taken from Caon et al. (2000) and (2) isophotes from the *Chandra* X-ray images superimposed on an optical image from the Digital Sky Survey.

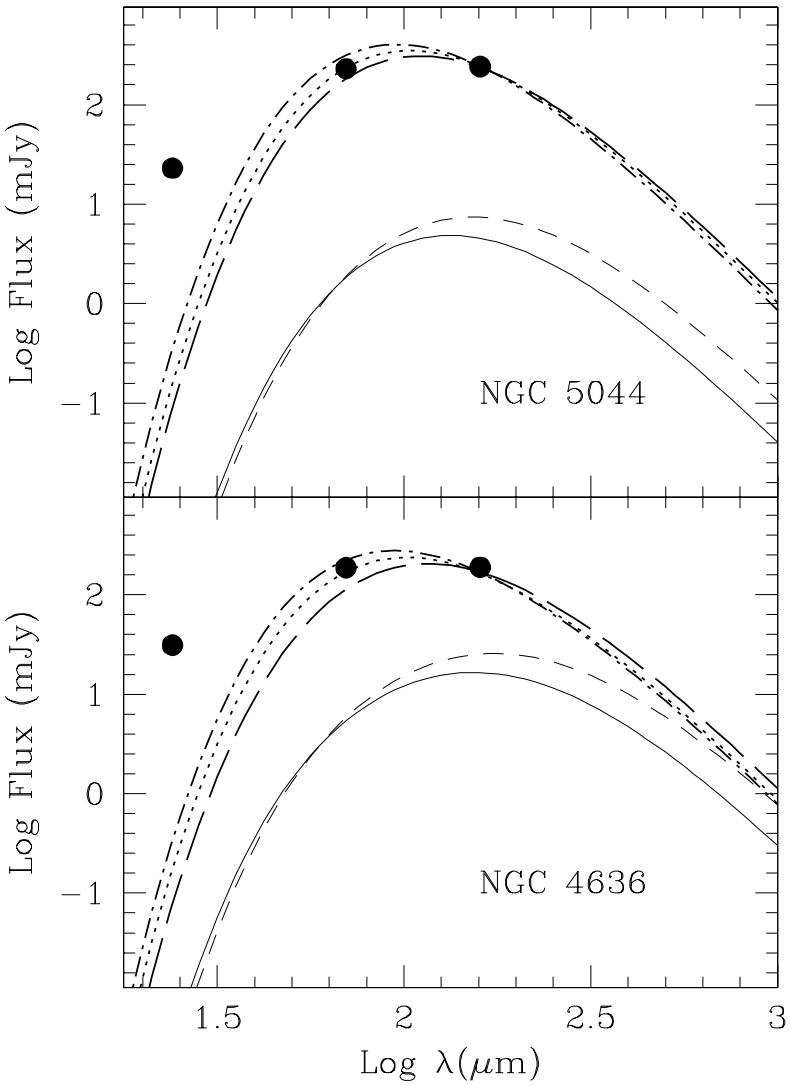

FIG. 3.— Solid circles show *Spitzer* MIPS flux observations for NGC 5044 and 4638 at 24, 70 and 160 μm. The lower two thin curves show the far-infrared steady state dust SED expected from normal stellar mass loss balanced by sputtering destruction in the hot gas. The short-dashed and solid lines show the SED based on initial grain size distributions with maxima at $a_{max} = 1$ and 0.3 μm respectively. These models are clearly insufficient to explain the observations of either galaxy – an additional source of extended dust is required. Each panel shows several models of the dust SED with extra dust, designed to fit the interstellar 70 and 160 μm fluxes (but not 24 μm which is circumstellar). As explained in the text, these models are characterized by two parameters (f_α, r_{ex}) which have the following values: *Upper panel:* (300,5kpc) (*dotted line*), (165,10kpc) (*long-dashed line*), (800,2kpc) (*dash-dotted line*); *Lower panel:* (60,4kpc) (*dotted line*), (26,10kpc) (*long-dashed line*), (133,2kpc) (*dash-dotted line*).

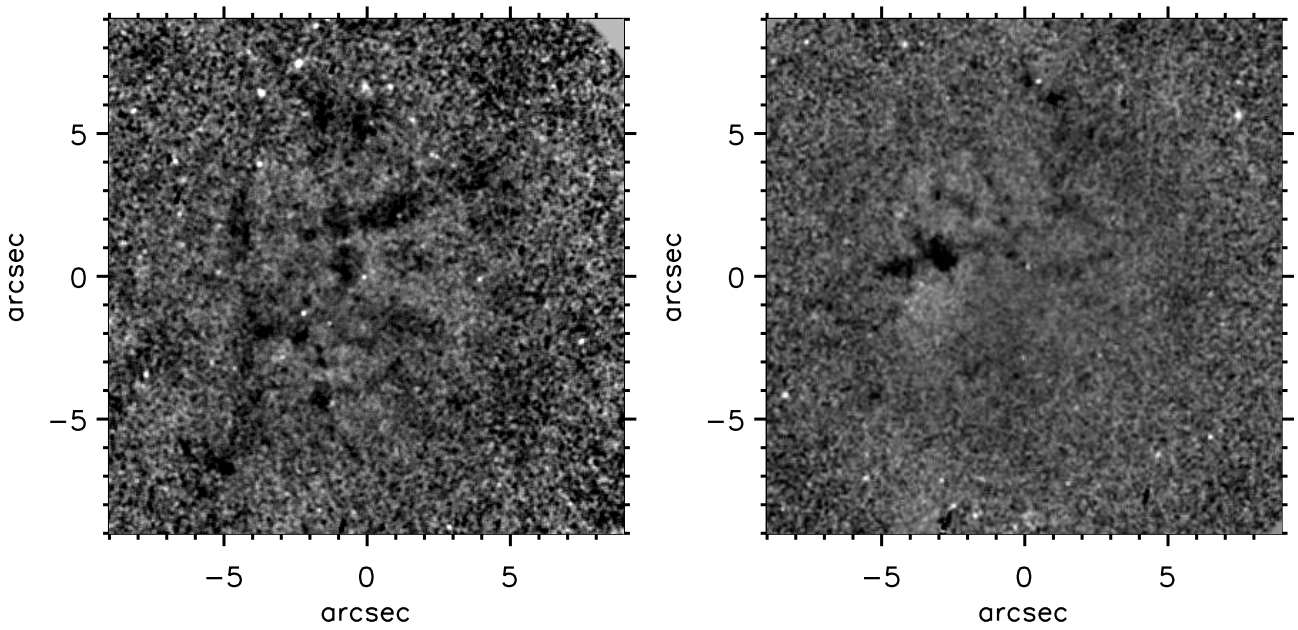

FIG. 4.— *Hubble Space Telescope* images of the central $\sim 1-2$ kpc in NGC 5044 (left panel) and 4636 (right panel). The optical dust maps were generated from archival HST data recorded with the Wide Field and Planetary Camera 2 (WFPC2) using the broad-band filters F791W and F547M. We first modeled the stellar contribution, recorded in the broad–band image, with elliptical isophotes using a two pass procedure to properly mask out and remove bad pixels and background/foreground objects. The dust map was then generated from the ratio of the continuum image over its purely stellar isophotal model. Dust absorption features are evident as dark filamentary structures in the maps.

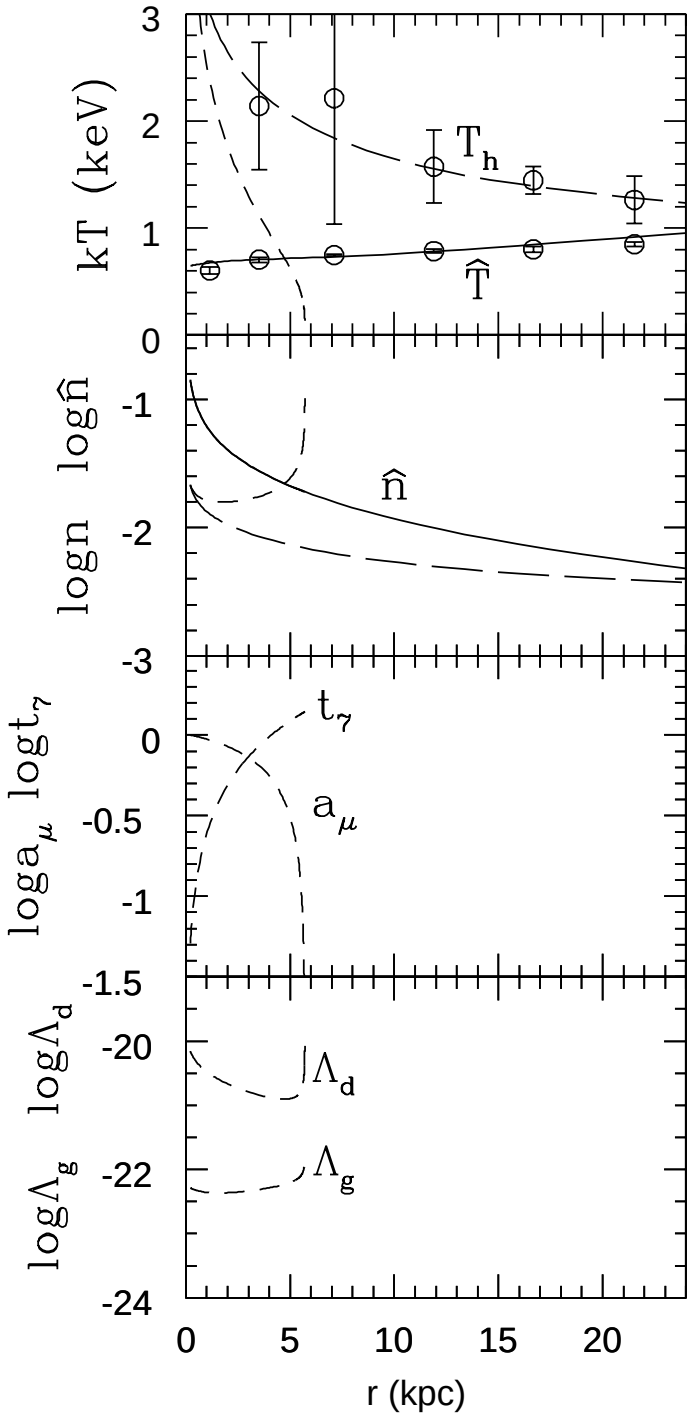

FIG. 5.— Approximate radial evolution of dust cooling in the constant-velocity buoyant outflow in NGC 5044. *Top panel:* temperature (K) of a dust-free buoyant element (long-dashed line) and dust-filled buoyant element (short-dashed line) compared to that of the ambient gas (solid line), *Second panel:* electron density (cm^{-3}) of the buoyant element (long-dashed line) compared to that of the ambient gas (solid line) and that in dusty buoyant gas (short-dashed line), *Third panel:* time t_7 in 10^7 yrs for the buoyant element to reach each radius (short-dashed line), radius a_μ of the grains in microns (short-dashed line), *Bottom panel:* radiative cooling coefficient Λ_{gas} (lower short-dashed line) and dust-assisted cooling coefficient Λ_{dust} (upper short-dashed line), both in erg cm^3 s^{-1}.

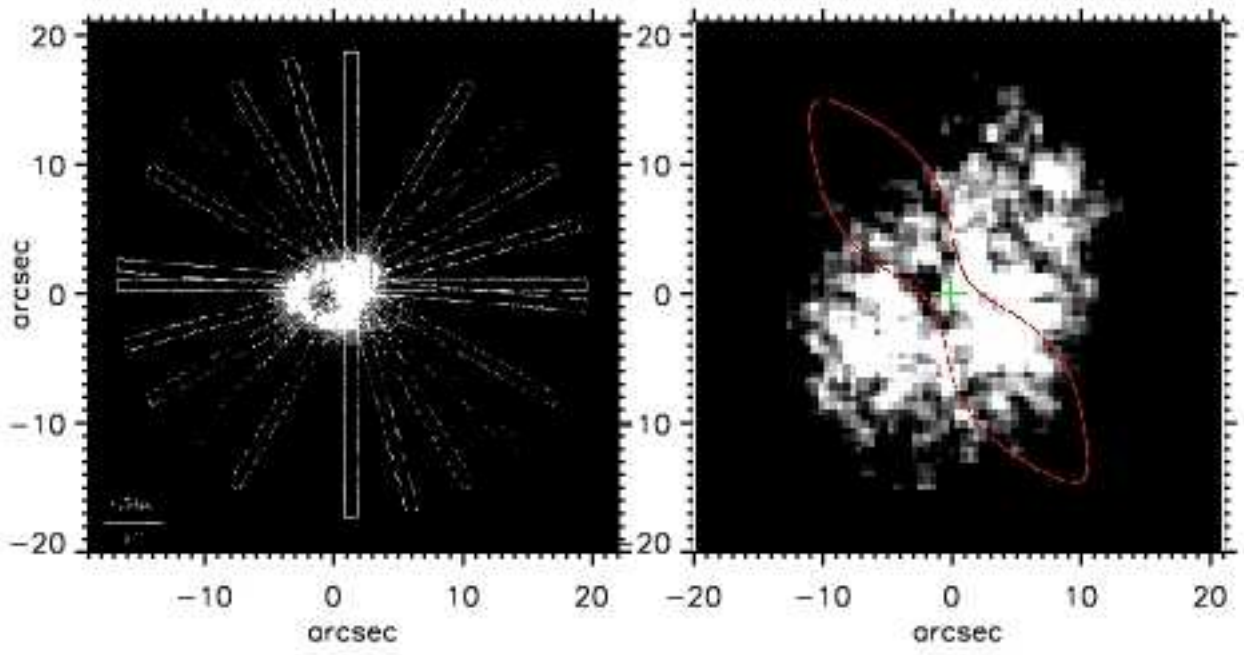

FIG. 6.— *Left Panel:* An Hα+[NII] image of NGC 4636 from Zeilinger et al. (1996) also showing the orientation of their slit spectra. These authors note that the slits are centered about 1.5″ from the galactic center. *Right Panel: Chandra* X-ray image from the *Chandra* archives with approximate radio contours of the double jet based on Birkinshaw & Davies (1985) and Stanger & Warwick (1986). The contours are symmetric about the green cross that shows the position of the galactic center based on a compromise between images from the Digital Sky Survey and the centroid of the HST stellar image.